Photon–Surface-Plasmon Coupling in Thick Ag Foils*

S. N. JASPERSON† AND S. E. SCHNATTERLY
Joseph Henry Laboratories of Physics, Princeton University, Princeton, New Jersey 08540
(Received 24 April 1969)

Photon–surface-plasmon coupling is observed in measurements of the optical reflectance of thick vapor-deposited Ag foils. Measurements of the surface-plasmon wave vector demonstrate that the optical excitation of the mode is an indirect process, the coupling mechanism providing the majority of the surface-plasmon momentum. Several experiments are performed in order to distinguish between various possible mechanisms, and only the surface roughness of the foil is found to contribute significantly to the observed interaction. The real and imaginary parts of the frequency-dependent dielectric response function are computed from the ellipsometry data of several foils. The surface-plasmon contribution appears as a resonant excess absorption in the imaginary part of the response, rising as much as 50% above the background level in the cases considered. The response of one foil is computed from data taken at two different angles of incidence in an attempt to observe the nonlocal nature of the portion of the absorption due to the surface-plasmon mode.

I. INTRODUCTION

THE discovery of surface-plasmon radiation emanating from electron-bombarded thick metal foils has stimulated considerable interest in the possible mechanisms which could, in fact, explain coupling between photons and the surface-plasmon mode of the conduction electrons in the metal. Ferrell[1] was the first to recognize that collective excitations in thin foils could decay by photon emission because of their slightly transverse nature required by the boundary conditions, and his predictions concerning specific properties of this radiation were soon verified experimentally.[2] However, his calculations still precluded the possibility that either surface- or volume-plasma oscillations in thick foils could radiate.

Ritchie and Eldridge[3] subsequently considered the more general problem of transition radiation, radiation created by the passage of a charged particle from one medium into another, and demonstrated that Ferrell's result was equivalent to theirs in the thin-foil limit at the plasma excitation energy. Several workers[4] obtained extended transition radiation spectra which were again in excellent agreement with theoretical predictions. Therefore, it was surprising when Boersch *et al.*,[5] exposing thick Ag foils to grazing-incidence electrons, observed the emission of intense radiation which could not be interpreted in usual terms. On the basis of the wavelength of the light and its dependence upon surface conditions, the source of the radiation was attributed to the decay of surface plasmons, although the coupling mechanism remained unknown. Jones *et al.*[6] soon verified these findings, but were reluctant to draw the same conclusions because the results of subsequent work[7] were again consistent with the existing theories.

In a second set of somewhat different experiments, several authors[8] found that photon-excited plasmons in thin Ag and K foils could radiate in directions other than the transmission and reflection directions of the incident light. Although the coupling of radiation polarized in the plane of incidence to the thin-foil plasmon mode was well understood,[9] the scattering of plasmons between excitation and decay was not.

Stern[10] proposed that the explanation in both cases was the presence of naturally occurring surface irregularities of dimensions comparable to a surface-plasmon wavelength. This roughness would in effect relax the requirement of momentum conservation between the plasmon and emitted photon, permitting the thick-foil surface plasmon to decay by photon emission and thin-foil plasmons to radiate in arbitrary directions.

* Work supported in part by grants from the National Science Foundation and the Research Corp.
† Present address: Department of Physics, University of Illinois, Urbana, Ill.
[1] R. A. Ferrell, Phys. Rev. **111**, 1215 (1958).
[2] W. Steinmann, Phys. Rev. Letters **5**, 470 (1960); R. W. Brown, P. Wessel, and E. P. Trounson, *ibid.* **5**, 472 (1960); E. T. Arakawa, N. O. Davis, and R. D. Birkhoff, Phys. Rev. **135**, A224 (1964).
[3] R. H. Ritchie and H. B. Eldridge, Phys. Rev. **126**, 1935 (1962).
[4] H. Boersch, C. Radeloff, and G. Sauerbrey, Phys. Rev. Letters **7**, 52 (1961); A. L. Frank, E. T. Arakawa, and R. D. Birkhoff, Phys. Rev. **126**, 1947 (1962); E. T. Arakawa, L. C. Emerson, D. C. Hammer, and R. D. Birkhoff, *ibid.* **131**, 719 (1963); E. T. Arakawa, N. O. Davis, L. C. Emerson, and R. D. Birkhoff, J. Phys. (Paris) **25**, 129 (1964); E. T. Arakawa, R. J. Herickhoff, and R. D. Birkhoff, Phys. Rev. Letters **12**, 319 (1964).
[5] H. Boersch, P. Dobberstein, D. Fritzsche, and G. Sauerbrey, Z. Physik **187**, 97 (1965). See also H. Boersch and G. Sauerbrey, in *Optical Properties and Electronic Structure of Metals and Alloys*, edited by F. Abelès (North-Holland Publishing Co., Amsterdam, 1966); P. Von Blanckenhagen, H. Boersch, D. Fritzsche, H. G. Seifert, and G. Sauerbrey, Phys. Letters **11**, 296 (1964).
[6] G. E. Jones, L. S. Cram, and E. T. Arakawa, Phys. Rev. **147**, 515 (1966).
[7] L. S. Cram and E. T. Arakawa, Phys. Rev. **153**, 455 (1967); J. C. Ashley, L. S. Cram, and E. T. Arakawa, *ibid.* **160**, 313 (1967).
[8] J. Brambring and H. Raether, Phys. Rev. Letters **15**, 882 (1965); W. Steinmann, J. Hofmann, and K. Stettmaier, Phys. Letters **23**, 234 (1966); P. Schreiber and H. Raether, Z. Naturforsch. **21a**, 2116 (1966); J. Bösenberg and H. Raether, Phys. Rev. Letters **18**, 397 (1967).
[9] R. A. Ferrell and E. A. Stern, Am. J. Phys. **30**, 810 (1962); A. J. McAlister and E. S. Stern, Phys. Rev. **132**, 1599 (1963).
[10] E. A. Stern, in *Optical Properties and Electronic Structure of Metals and Alloys*, edited by F. Abelès (North-Holland Publishing Co., Amsterdam, 1966), p. 396; E. A. Stern, Phys. Rev. Letters **19**, 1321 (1967).

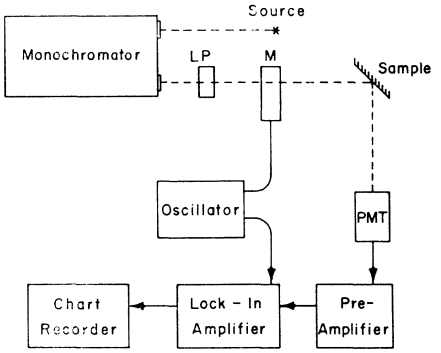

FIG. 1. Schematic diagram of the experimental system. LP is a linear polarizer, M is the polarization modulator, and PMT is the photomultiplier tube.

Teng and Stern[11] proceeded to confirm this theory in the thick-foil limit by observing anomalous radiation from electron-bombarded Al and Ag diffraction gratings which could only be explained as surface-plasmon radiation characteristic of the periodic surface irregularities due to the grating rulings. In the thin-foil case, Schreiber[12] found the intensity of scattered resonance radiation to correlate with the degree of surface roughness, the roughness being determined from electron-microscope pictures of the surface.

Additional theoretical investigations have explored the possibility that other mechanisms might also enable photon–surface-plasmon coupling in the thick-foil case. Ritchie[13] has shown that normal incidence photons can excite surface plasmons through the intermediary of intraband transitions. Fedders[14] has found that in a gas of interacting electrons there should exist a small, resonant contribution to the optical conductivity, hence reflectivity, centered at the surface-plasmon energy for light polarized parallel to the plane of incidence only. More recently, Fedders[15] has obtained quantitative estimates of the change in reflectivity to be expected due to coupling between incident light and surface plasmons via surface roughness, phonons, and impurities.

We have previously reported[16] the observation and identification of the surface-plasmon contribution to the optical reflectivity of thick, ostensibly smooth Ag foils. In this paper we shall present the details of that work, together with several additional optical experiments which allowed the unambiguous identification of surface roughness as the dominant coupling mechanism.

To recapitulate briefly before proceeding to experimental detail, the surface-plasmon mode of a bounded electron gas[17] exists at the frequency ω_{sp}, where the real part of the dielectric response function is equal to the negative of the dielectric constant ϵ_d of the bounding medium:

$$\epsilon_1(\omega_{sp}) = -\epsilon_d. \quad (1)$$

Implicit in this resonant condition is the assumption that the imaginary part of the dielectric response, ϵ_2, is much less than 1, so that the plasma oscillations are not heavily damped by one-electron excitations.

For many metals, Eq. (1) is satisfied at energies of the order of 10 eV. In the case of Ag, however, a *d*-band to Fermi-surface interband transition[18] with onset near 3.88 eV (3200 Å) causes ϵ_1 to increase rapidly and become positive (see Fig. 3, Ref. 19; or Fig. 14 of this paper) at a much lower energy than expected for a free-electron gas of comparable electron density. Since ϵ_2 is small in the region immediately below 3.88 eV (above 3200 Å), well-defined surface plasmons for $\epsilon_d = 1$ are expected to exist at an energy of 3.65 eV (3400 Å). This relatively low energy makes Ag particularly attractive for use in plasmon optical experiments, since it lies in the near ultraviolet, where quartz optics and standard photomultipliers function adequately. On the other hand, the proximity of the Ag transparency, $\epsilon_1 = 1$, just 0.2 eV away from the surface-plasmon resonant energy, presents an offsetting experimental difficulty, as any structure due to the surface-plasmon mode is apt to be obscured by the precipitous drop in reflectance[20] which occurs between 3.35 and 3.88 eV (3700 and 3200 Å).

This problem was alleviated by the development of a new experimental technique, which is outlined in Sec. II A. Other experimental considerations are presented in the remainder of Sec. II, and the results and related discussion are presented in the several subparts of Sec. III.

II. EXPERIMENTAL

A. Polarization Modulation

The experimental system used in the majority of this work is shown schematically in Fig. 1. Details of operation beyond that presented below can be found in Ref. 21.

Light from a 450-W xenon arc lamp is made monochromatic (10 Å half-width band pass) by a grating monochromator,[22] linearly polarized by a Polaroid HNP'B sheet polarizer (LP), polarization modulated by M, obliquely reflected by the sample, and detected by

[11] Ye-Yung Teng and E. A. Stern, Phys. Rev. Letters **19**, 511 (1967).
[12] P. Schreiber, Z. Physik **211**, 257 (1968).
[13] R. H. Ritchie, Surface Sci. **3**, 497 (1965).
[14] P. A. Fedders, Phys. Rev. **153**, 438 (1967).
[15] P. A. Fedders, Phys. Rev. **165**, 580 (1968).
[16] S. N. Jasperson and S. E. Schnatterly, Bull. Am. Phys. Soc. **12**, 399 (1967).
[17] E. A. Stern and R. A. Ferrell, Phys. Rev. **120**, 130 (1960).
[18] H. Ehrenreich and H. R. Philipp, Phys. Rev. **128**, 1622 (1962).
[19] R. H. Huebner, E. T. Arakawa, R. A. MacRae, and R. N. Hamm, J. Opt. Soc. Am. **54**, 1434 (1964).
[20] See Fig. 1, Ref. 19.
[21] S. N. Jasperson and S. E. Schnatterly, Rev. Sci. Instr. **40**, 761 (1969).
[22] Spex Industries, Inc., 1700 ¾-Meter Czerny-Turner spectrometer with a 1200 1/mm grating.

an EMI 9558Q photomultiplier tube (PMT). In brief, a periodic, uniaxial strain induced in a normally isotropic quartz block M causes the state of polarization of the light, initially linearly polarized at an angle to the strain axes, to be modulated at the frequency of strain modulation, 50 kHz. For a suitable modulation level and orientation of the optical elements, the plane of polarization of the light emergent from M can be made to lie alternately perpendicular and parallel to the plane of incidence of the sample, thus causing a modulation of the reflected intensity proportional to (R_s-R_p).

The subsequent ac component of the PMT output current is amplified and fed into a Princeton Applied Research JB-5 lock-in detector, which demodulates the signal and records it on a Moseley Autograf Chart recorder. The reference signal required by the lock-in detector is obtained from the oscillator which drives the modulation unit.

Important subsidiary units not shown in the diagram are: (1) a control circuit coupled to the PMT high-voltage supply, which maintains the average PMT output current at a constant value, thus normalizing the ac component so that it is proportional to the ratio $(R_s-R_p)/(R_s+R_p)$; and (2) a circuit which couples the oscillator amplitude adjustment to the wavelength drive of the monochromator, thus fixing the degree of polarization modulation at a constant level, independent of the wavelength. These units facilitate the direct interpretation of data measured as a continuous function of the wavelength: the lock-in amplifier output voltage at each wavelength is simply equal to $(R_s-R_p)/(R_s+R_p)$ times a constant of proportionality which can be specified by a calibration measurement at any point within the range.

For convenience of notation, we introduce a normalized reflectance difference parameter N,

$$N=(R_s-R_p)/(R_s+R_p)\,. \tag{2}$$

According to this definition, N becomes zero at both $\theta=0$ and 90° angle of incidence, since at these angles R_s and R_p are equal, irrespective of the properties of the reflecting surface. N attains its maximum value at the pseudo-Brewster angle, which in the case of high-reflectivity metals is generally very nearly 90°. In all situations encountered, however, N measured at $\theta=45°$ was of the same order of magnitude as the maximum value of N, so for experimental convenience the angle of incidence was fixed at 45°. The fact that N in this high-reflectivity regime is a small quantity, typically of order 0.01, poses no experimental difficulty since the detection scheme described above is capable of measuring $N\geq 0.01$ with 1% accuracy. Furthermore, the differential nature of N causes it to be more sensitive to small changes in the dielectric response of the reflecting medium than are the individual reflectances R_s and R_p measured with comparable accuracy.

B. Reflectance Modulation

A second modulation technique, similar to that described by Beaglehole,[23] was used during one set of experiments in order to measure quantities related to the individual reflectances R_s and R_p, rather than their composite function N. With reference again to Fig. 1, the polarization modulator (M) is removed from the optical path and the sample mount is replaced by a turntable which rotates at 50 rps. The turntable supports a 2-in.-diam optically polished quartz disk and is so positioned that the light beam intercepts the disk near its rim. Foils of two different materials are condensed on alternate octants of the quartz disk by the appropriate masking of its surface during two vapor depositions. Hence, as the turntable spins, the light beam is alternately reflected by the two materials at four times the frequency of rotation, 200 Hz, thus giving rise to an intensity modulation proportional to the difference between the reflectances of surface 1 and surface 2, R_1-R_2.

The output of the detection system, as before, is proportional to

$$N'=(R_1-R_2)/(R_1+R_2)\,, \tag{3}$$

which is most sensitive to reflectance changes when $R_1\simeq R_2$. If this approximate equality holds and, in addition, one of them (R_2) is essentially wavelength-independent, then wavelength-dependent changes in R_1 are directly proportional to changes in N':

$$\Delta R_1\simeq 2R_2\Delta N'. \tag{4}$$

The component of R_1 to be analyzed is selected by orienting the axis of polarizer LP either parallel or perpendicular to the plane of incidence of the surface, and the angle of incidence θ is arbitrary. The lock-in detector reference signal is derived from the detection of an auxiliary light beam which is chopped by the turntable at 200 Hz. The initial calibration of the detection system was made with reference to a disk supporting alternate octants of vapor-deposited Al and flat black paint.

C. Sample Preparation

All Ag samples used in this work were prepared by vapor-deposition at pressures of approximately 1.10^{-6} Torr Ag of 99.999% purity was evaporated from a molybdenum boat onto glass microscope slides to thicknesses of 1000–4000 Å at rates of 100–300 Å per sec.

Experience indicated that the sample properties were not sensitive to the choice of methods used to clean the substrates; therefore, the glass slides were simply washed with detergent, rinsed in distilled water, and dried just prior to placement in the vacuum system.

[23] D. Beaglehole, Appl. Opt. 7, 2218 (1968); D. Beaglehole and T. J. Hendrickson, Phys. Rev. Letters 22, 133 (1969).

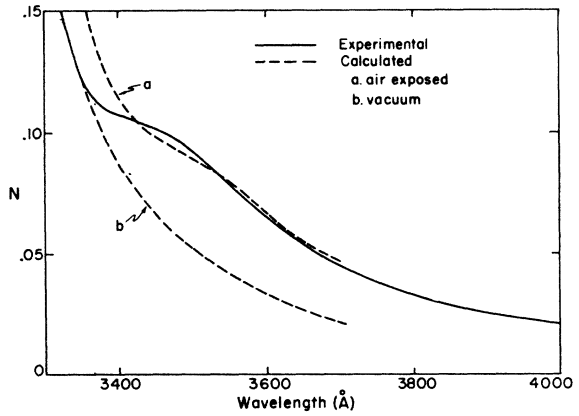

FIG. 2. N versus wavelength: experimental and calculated.

The boat and its contents were thoroughly outgassed prior to each evaporation by slowly raising the boat temperature to a point where the Ag was just beginning to evaporate. The substrates were shielded during this procedure by a mechanically controlled baffle which could be swung in between the boat and the subtrates. Deposition was not begun until the pressure in the chamber returned to its base level.

During the deposition, the foil thickness was monitored by a quartz oscillator thickness measuring device[24] located next to the substrates. The deposition rate was obtained indirectly by dividing the film thickness by the time required for deposit. A rather rapid rate was sought in accordance with the work of other authors,[25] which indicates that this condition favors better film formation. The substrates were assumed to remain near room temperature throughout the evaporation, and annealing of the foils was not attempted at any time during the experiment.

Samples were removed from the vacuum chamber within minutes after evaporation and either placed in the experimental apparatus for immediate study or stored in a $CaCl_2$ desiccator to await study at a later time.

III. RESULTS AND DISCUSSION

A. Dielectric Dependence

A graph of N, typical of the majority of thick-foil chart recordings made in the course of this work, is shown as a solid curve in Fig. 2. It is characterized by a small magnitude at the long-wavelength end, a sharply increasing slope and magnitude toward the short-wavelength end, and a rather significant resonant structure centered at approximately 3450 Å. Noise was of negligible consequence due to the properties of the detection technique: The standard deviation of the raw trace from a smooth curve, such as that replicated above, was 0.3% of the magnitude of N. In addition, the wavelength-dependent systematic errors were less than 1% of N throughout this range, permitting resolution of structure considerably smaller than that observed near 3450 Å.

Except for this resonant structure, the differential reflectance is qualitatively similar to what one would expect from a classical free-electron gas with $\epsilon_1=0$ at 3300 Å and $\epsilon_2<1$. For comparison with previously obtained experimental data, computer-generated curves of N derived from the dielectric constants quoted by Huebner *et al.*[19] are shown as dashed curves in Fig. 2, curve (a) corresponding to data obtained with air-exposed Ag foils, and (b) to data obtained with samples which remained in a vacuum throughout the preparation and measurement. Curve (b) is structureless in agreement with free-electron-like behavior and matches the solid curve below 3350 Å, whereas (a) is considerably displaced, closely matching the present data above 3400 Å, and possesses at least a hint of a resonance.

Although the proximity of the resonance to the wavelength where $\epsilon_1=-1$ suggests a surface-plasmon contribution to the reflectance, the difference between curves (a) and (b), showing that air exposure can produce significant changes in sample properties in the range of interest, caused initial concern that the 3450-Å structure was the result of surface contamination. A computer program was written which demonstrated that a surface dielectric layer with an absorption band of moderate strength could easily account for the resonance, even if the layer were only 10 or 20 Å thick. This sensitivity to contamination thickness agreed well with an early observation that the strength of the resonance varied measurably from one sample to the next.

The resonant condition specified by Eq. (1), however, provides a unique criterion for establishing the identity of the surface-plasmon mode, since no other absorption mechanism in a substance could be dependent upon the polarizability of the bounding medium. This suggests placing a transparent dielectric in contact with the Ag

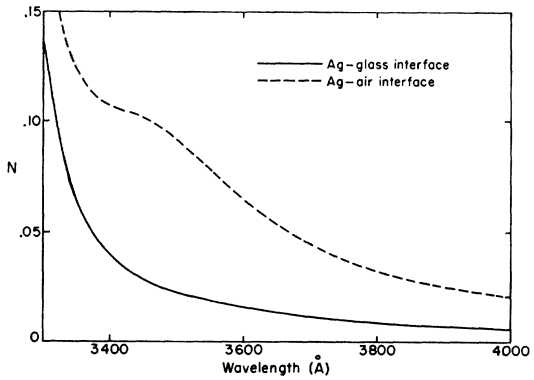

FIG. 3. Comparison of results: Ag-glass interface (solid line), and Ag-air interface (dashed line).

[24] Sloan Instruments Corp., Model DTM-3.
[25] R. S. Sennett and G. D. Scott, J. Opt. Soc. Am. **40**, 203 (1950); G. Hass, *ibid.* **45**, 945 (1955).

foil and looking for a subsequent relaxation of the resonance to a longer wavelength. Such a test appeared trivial, since glass is transparent to light of wavelengths longer than 3300 Å, making it possible to turn the samples around and view the Ag-glass interface through the glass substrate. If the resonance were due to the surface plasmon mode, it would shift to approximately 3600 Å, the predicted resonant wavelength for $\epsilon_d \simeq 2$.

Figure 3 shows a graph of N obtained from the Ag-glass interface; the corresponding Ag-air recording is shown as a dashed line for comparison. The uniformly smaller magnitude of the solid curve is consistent with the anticipated effect of the thick glass substrate, but clearly no resonance now exists, either at 3450 or 3600 Å. This result was duplicated with each of over two dozen other samples, some of which were deposited on quartz, cleaved wafers of NaCl, and mechanically roughened glass substrates.

These negative results soon made it apparent that a better test would be the placement of a dielectric layer in contact with a front surface already exhibiting a resonance. Since it seemed desirable that the dielectric have as little effect as possible on the Ag surface, while still conforming to every contour, water was chosen for the initial attempt.

In order to perform this experiment, a water-tight pocket with a quartz front face was constructed which held the sample in the beam in its customary orientation. First, a recording of N was taken with the sample in the pocket, but with no water present. Except for a slight vertical shift of the whole recording due to the quartz window, the results were similar to previous Ag-air graphs. Next, without disturbing the physical arrangement of the system, a few drops of distilled water were placed in the pocket so as to completely fill the 1-mm space between the Ag foil and the window of the pocket, and a second recording over the same range was taken. Finally the water was drained away, and the pocket and foil were thoroughly dried by a stream of helium gas. A few minutes later a third recording was taken.

Figure 4 shows the results of one such series, where curves (a), (b), and (c) correspond, respectively, to the first, second, and third scans discussed above. The results provide the conclusive proof that the surface-plasmon mode is responsible for the resonant structure: The resonance clearly has been shifted 100 to 150 Å by the presence of water, as required by Eq. (1), for $\epsilon_d = 1.8$.

A second feature illustrated by Fig. 4 is the effect aging has on the Ag foils. The sample under consideration was made 44 days before this experiment and stored in a desiccator throughout the period, except for a matter of hours when used in other experiments. A recording of N taken shortly after the sample was made is shown as a dashed line for comparison. The large increase in curve (a) is apparently due to surface

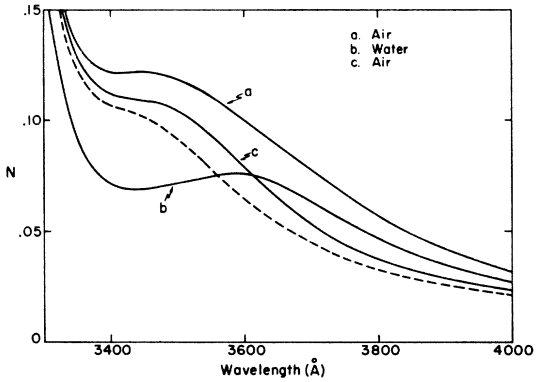

FIG. 4. Dielectric relaxation of the surface-plasmon resonance. The solid lines were obtained with a 44-day-old sample; the dashed line was obtained with the same sample minutes after it was made.

contamination formed during storage which partially dissolved or washed away in the water between recordings (a) and (c). In the case of similar experiments performed with newly prepared foils, curves (a) and (c) were essentially identical.

Stern and Ferrell[17] have considered the situation in which the dielectric layer is of finite thickness (vacuum occupying the remainder of space) and found the resonant condition to be

$$\epsilon_1(\lambda_{sp}) = -\epsilon_d\left(\frac{1+\epsilon_d \tanh kt}{\epsilon_d+\tanh kt}\right), \tag{5}$$

where ϵ_1 is now expressed as a function of wavelength to conform with the units of data presented in this paper, k is the magnitude of the surface-plasmon wave vector, and t is the dielectric film thickness. Therefore, it is evident that the dominant wave-vector magnitude can be determined by measuring the fractional shift of the resonance wavelength as a function of dielectric thickness.

Very thin layers would be required, however: A 200-Å film of $\epsilon_d = 2$ would shift the resonance 50%, assuming a $\mathbf{k}$ vector of the same order of magnitude as that of the light. Consequently, something more manageable than water is required, and an effort was made to vacuum-deposit thin layers of solid dielectric on top of Ag foils, using the evaporation techniques of Section II C. MgF_2, which is transparent throughout this wavelength range and has a dielectric constant of 1.93,[26] was found to work satisfactorily. The average film thickness was measured as usual by the quartz oscillator thickness monitor, which could be read to ± 3 Å for films of a few dozen angstroms thickness. Since the samples were mounted adjacent to the monitor so as to have the same view of the evaporation source, it was assumed that the average thickness measured by the monitor and that actually deposited

[26] A. Duncanson and R. W. H. Stevenson, Proc. Phys. Soc. (London) **72**, 1001 (1958).

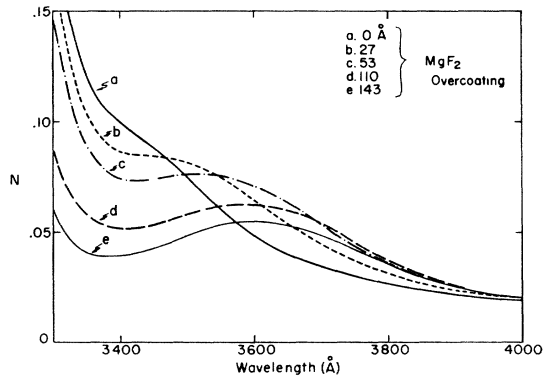

FIG. 5. Resonance position versus thickness of MgF_2 overcoating.

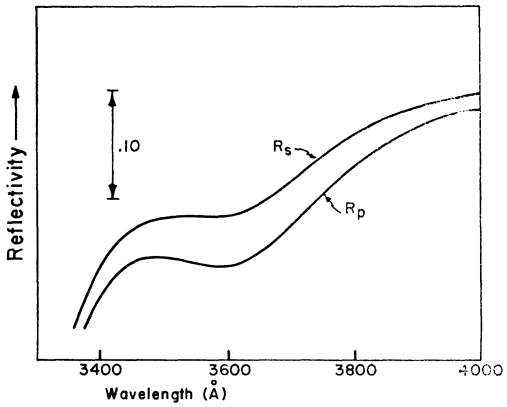

FIG. 6. Relative reflectivity of Ag: 45° angle of incidence.

on the samples were equal to within experimental error. No attempt was made to study the uniformity of the deposited layer.

The experiment proceeded as follows. An initial recording of N was obtained from a fresh Ag sample within minutes after film deposition. The sample was then placed back in the evaporation chamber, overcoated with a MgF_2 layer of approximately 30 Å thickness, and returned to the optical bench for a second N recording. This process was repeated several times, always with the addition of the same thickness increment of dielectric, until the resonance was completely shifted. Care was taken prior to each recording to ensure that the sample was returned to the same orientation on the optical bench.

The composite results of such a series in which the thickness increment was 27 Å is shown in Fig. 5. These graphs indicate that one 27 Å layer shifts the resonance by approximately 33%, and that a thickness of 110 Å or more shifts the resonance to its completely relaxed position.

According to both the dielectric constant data of Huebner *et al.*[19] and those reported in Sec. III E, ϵ_1 is approximately a linear function of the wavelength between 3400–3600 Å. If it is assumed that $\epsilon_1(3450\text{ Å}) = -1.0$ and $\epsilon_1(3600\text{ Å}) = -1.93$ on the basis of the initial and final resonance positions observed in Fig. 5, Eq. 5 can be inverted to solve for kt in terms of the percentage shift from initial to final position. From the results shown in Fig. 5, plus two similar sets of recordings, the wave-vector magnitude was calculated to be $(1.1\pm0.3)\times10^6$ cm^{-1}. This rather large spread in values is due to the difficulty in accurately specifying the central resonance wavelength: The resonance is initially situated on a steeply sloped background, and its half-width is larger than the total shifted distance.

In Sec. III E, evidence is presented which suggests that the unshifted position is actually 3400 rather than 3450 Å, and that apparently the resonance is partially relaxed by a thin corrosion layer even before the first recording can be made. Solving the new boundary valued problem and proceeding as above, with the added assumption that the dielectric constant of the corrosion layer is between 2 and 4, we find this situation still to be consistent with a wave vector of approximately 1×10^6 cm^{-1} and that it implies a corrosion layer of 20–24 Å thickness.

Therefore, all experimental evidence points toward a magnitude of 1×10^6 cm^{-1} for the dominant wave vector of the surface plasmon. In contrast, the magnitude of the projection of the wave vector of 3450 Å light in the plane of the surface is only 1.3×10^5 cm^{-1}, a factor of 8 smaller. We are thus able to compare directly the momentum of the incident photon with that of the outgoing surface-plasma wave and demonstrate that they are not equal for this indirect optical-absorption process.

B. Polarization and Angular Dependence

In order to measure the effect of the surface-plasmon mode on the individual reflectances R_s and R_p, the optical system was temporarily modified as described in Sec. II B. Ag was deposited on alternate octants of the quartz disk, Al on the remaining octants. Since the reflectance of Al is nearly equal to that of Ag at 4000 Å and essentially wavelength-independent between 3000 and 4000 Å, Eq. (4) is valid: The reflectance of Ag is directly proportional to N', the output of the detection system.

Graphs of R_s and R_p measured at $\theta=45°$ are shown in Fig. 6. The Ag octants in this case were overcoated with 150 Å of MgF_2 to make the resonance more visible, and it is apparent that light of both polarizations couples strongly to the surface-plasmon mode. The resonance is visible in N as well simply because the coupling strengths in R_s and R_p are slightly different. The intercept of both curves with the vertical axis at 4000 Å is presumed to be approximately 0.9, but since no absolute reflectance measurement was made, only a relative vertical scale is shown.

Similar recordings of R_s and R_p were made for $\theta=7°$ and are plotted as a single solid curve in Fig. 7, since

the difference between the two was negligible. Again the resonance shows up strongly, apparently having little dependence upon the incident angle of the light. To illustrate the obscurity of the resonance in the ordinary reflectivity, we present, as a dashed line in Fig. 7, the graphs of R_s and R_p obtained before the addition of the MgF_2 overcoating. Although the surface-plasmon contribution to the reflectivity is large, it is almost completely hidden by the sharp drop in reflectance caused by the Ag transparency.

At this point it is convenient to summarize what can be said concerning the various coupling mechanisms in view of the experimental facts. Ritchie's theory[13] involving intermediate intraband transitions clearly does not describe the observed phenomenon, since it predicts an absorption edge rather than a resonant line shape. Likewise, Fedders's theory[14] involving nonlocal conductivity is not adequate, since it predicts no resonance in R at normal incidence or in R_s at any angle of incidence, whereas a resonance is observed experimentally in both instances. Therefore, the only anticipated mechanisms still remaining are phonons, impurities, and surface roughness.

C. Temperature Dependence

The fact that observed resonances in room-temperature recordings of N were found to vary greatly in strength from sample to sample is in itself preliminary evidence that the coupling is not due to phonons, because of the unlikelihood that such a mechanism would be so sensitive to sample properties. Further evidence to this effect was obtained by measuring the resonance size as a function of temperature between 100–300°K.

The expression for the probability of a photon excitation of a surface plasmon accompanied by the simultaneous absorption or creation of a phonon is identical in form to that describing indirect optical absorption in semiconductors,[27] the only physical difference being that a collective, rather than single-particle, mode is being excited. The temperature dependence of the probability is proportional to $\coth(E_{ph}/k_BT)$, where E_{ph}, k_B, and T are the phonon energy, Boltzmann constant, and absolute temperature, respectively. Since the wave-vector magnitude of the phonons must be approximately equal to that measured for the surface plasmons, a quantity two orders smaller than the wave-vector magnitude at the zone boundary, a reasonable approximation for the phonon energy is

$$E_{ph}=\hbar k_{ph}v_{ph}, \tag{6}$$

where k_{ph} is the phonon wave-vector magnitude and v_{ph} is the velocity of sound in Ag, 3×10^5 cm/sec.[28]

[27] R. A. Smith, *Wave Mechanics of Crystalline Solids* (John Wiley & Sons, Inc., New York, 1961).

[28] C. Kittel, *Introduction to Solid State Physics* (John Wiley & Sons, Inc., New York, 1965), 2nd ed., p. 100.

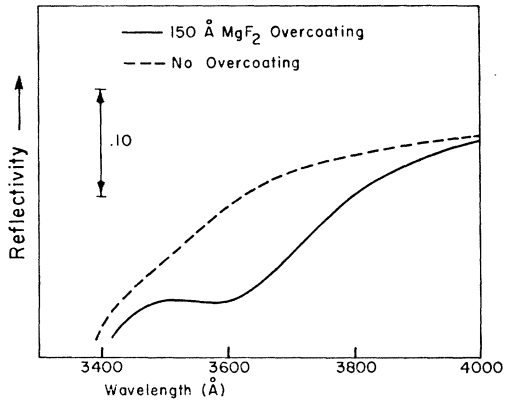

FIG. 7. Relative reflectivity of Ag: 7° angle of incidence. The solid line corresponds to a sample overcoated with 150 Å of MgF_2; the dashed line to an untreated sample.

This energy, 2×10^{-4} eV, is equal to k_BT for $T=3$°K, allowing one to expand $\coth(E_{ph}/k_BT)$ in the high-temperature limit,

$$\coth(E_{ph}/k_BT)=k_BT/E_{ph}, \tag{7}$$

for the temperature range used in the experiment. Therefore, the probability for phonon-assisted excitations should be directly proportional to the temperature.

In order to examine the actual temperature dependence, a sample was placed in thermal contact with a liquid-nitrogen Dewar and mounted inside a vacuum chamber. Quartz windows in the chamber allowed optical access for the usual recordings of N at $\theta=45°$. A thermocouple located on the sample mount monitored the temperature which was varied by pouring small amounts of liquid nitrogen into the Dewar. Several recordings were made between room temperature and 110°K, the lowest temperature accessible with this system. This method of cooling was nondestructive to the Ag foils: Recordings at 290°K before and after cooling were always identical.

All samples used in this work were first overcoated with 150 Å of MgF_2, both to make the resonance more visible and to prevent further relaxation due to a layer of ice which always formed on the sample surface as soon as the temperature fell below 0°C. Initial attempts toward eliminating the ice formation proved futile; however, it was found that by cooling the sample past 0°C very slowly, the effect of the ice was limited to a uniform vertical displacement of the N recordings without the addition of spurious structure in the vicinity of the surface-plasmon resonance.

Graphs obtained at 290 and 110°K are shown in Fig. 8, where the absolute value of the ordinate and relative placement of the two graphs remains unspecified because of the contribution of the ice layer. It is observed that the strengths of the resonances at the two temperatures are the same to within the accuracy of the experiment. Results of two similar trials indicated

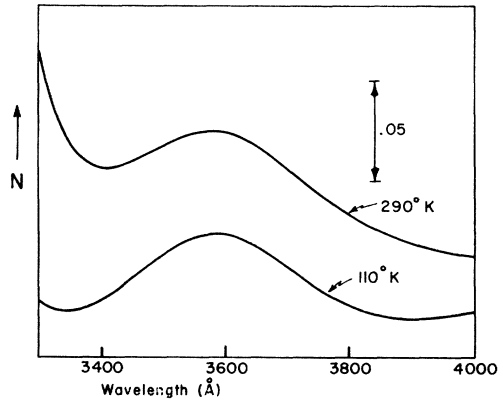

FIG. 8. Temperature dependence of the resonance.

the same lack of temperature dependence. Over this same temperature range, however, the probability of phonon-assisted excitation should change by a factor of 3. Although it would be preferable to perform this experiment in a better vacuum where effects of the ice layer could be avoided, these results suffice in eliminating the possibility that phonon-assisted coupling contributes significantly to the photon–surface-plasmon coupling.

D. Surface Roughness

It may be recalled that, once the observed resonance in N was properly identified, the consistent lack of a resonance at the Ag-substrate interfaces provided an initial indication that surface conditions of the foil are crucial to photon–surface-plasmon coupling. This suggested altering the substrates in various controlled ways to investigate the dependence upon surface roughness.

At the outset it was not clear whether glass substrates were too smooth or too rough to permit coupling. As stated above, several different substrates and substrate conditions had already been tried, all with the same lack of success.

The first successful substrate modification came as a result of overcoating a glass slide with approximately 2000 Å of MgF_2 prior to the Ag deposition. Subsequent recordings of N are shown in Fig. 9, where solid curves (a) and (b) are the Ag-substrate recordings of two samples which were made simultaneously: Foil (a) was deposited on a MgF_2 overocated substrate; foil (b) on a plain glass substrate. The resonant structure in (a) is clearly reminiscent of those observed earlier at the Ag-air interface.

In order to ensure that this resonance in (a) was not in part due to interference effects in the thin MgF_2 layer, a computer program was written to evaluate the reflectance of such a multilayer system, summing multiply reflected amplitudes in the Ag and MgF_2 layers and multiply reflected intensities in the glass substrate. The results indicated that the reflectance has negligible dependence upon the thickness of the MgF_2 for Ag foils greater than 1000 Å thick. In addition, the program was used to calculate graphs of N which would be observed from such a system, assuming that the dielectric constants presented in the Sec. III E specified the response of these foils at the Ag-glass and Ag-MgF_2 interfaces. The lower dashed curve in Fig. 9 was obtained with the dielectric constants of sample 5. (See Figs. 12–14), modified by subtracting the surface-plasmon resonance from the graph of ϵ_2 so that only a smooth background remained; the upper dashed curve was obtained with the same values, modified by adding the ϵ_2 surface-plasmon resonance back in, but now with its center at 3600 Å. Although the two dashed curves do not coincide with their solid-line counterparts, it is apparent that the two sets are very similar: No resonance exists at the Ag-glass interface in foil (b); a rather substantial, shifted resonance exists at the Ag-MgF_2 interface in foil (a).

Similar pairs of samples were made with a variety of Ag foil thicknesses between 400 and 4000 Å. For all pairs of thicknesses greater than 1000 Å, the results were similar to those illustrated in Fig. 9; for thicknesses less than 1000 Å, interference effects in the MgF_2 and Ag films obscured the resonance, so that comparison between plain and overcoated substrates was impossible.

In another series of experiments, the glass itself was roughened on a more microscopic scale than was possible mechanically by exposing it to a vapor of hydrofluoric acid. Several glass slides were prepared for study, each exposed to the vapor for a different length of time so that the amount of pitting varied from one substrate to another. Only one surface of each slide was roughened; the second side was protected by a layer of wax, which was removed during the cleaning process prior to deposition of the Ag foil.

Ag-glass recordings of N from one such set of samples are shown in Fig. 10. Curve (a) was obtained from an untreated reference sample; substrates correspond-

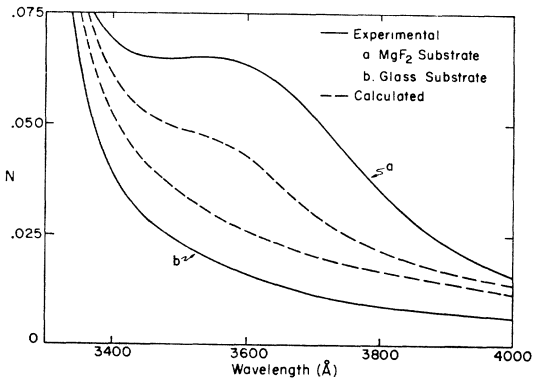

FIG. 9. Comparison of results: Ag-MgF_2 interface (a) and Ag-glass interface (b). Computer-calculated curves are shown as dashed lines.

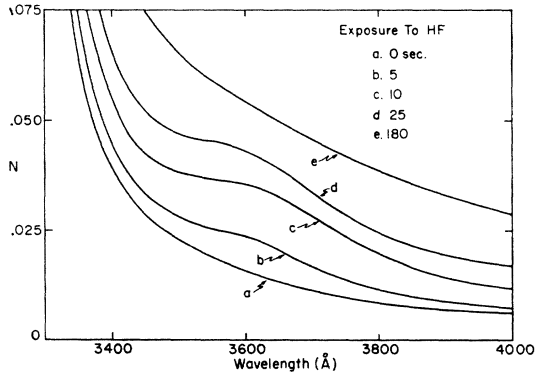

FIG. 10. Results obtained with acid-roughened substrates: Ag-glass interface.

ing to curves (b), (c), (d), and (e) were exposed to the vapor for 5, 10, 25, and 180 sec, respectively. The absolute time duration is not significant, since the vapor density depends upon the details of the method of exposure. The relative exposure lengths, however, should correlate with the relative degree of surface roughness, and in fact curves (b) through (e) are seen to be uniformly displaced from curve (a) by progressively larger amounts. In addition, a resonance centered at 3600 Å is observable in the recordings corresponding to intermediate exposures. Presumably, none is visible in (e) because of heavy damping of the mode due to the extremely rugged surface.

These results are rather conclusive proof that surface roughness is the dominant coupling mechanism. They would suggest that untreated glass slides are too smooth (or at least improperly rough) to allow coupling at the Ag-glass interface, whereas the opposite, free surface of thick foils tend to form with a spontaneous roughness which is usually suitable for optical observation of the surface-plasmon mode. Overcoating the slides with a 2000 Å layer of MgF_2 creates a substrate surface of a more suitable roughness, as does briefly exposing the glass surfaces to HF vapor. Comparison of Figs. 9 and 10 indicates further that the first method of altering the substrate is somewhat more effective than the second. On the other hand, resonances observed at the Ag-air interface of foils deposited on certain HF-roughened substrates were the largest observed in the course of the entire work. The five graphs in Fig. 11 illustrate this tremendous variation in the magnitude of Ag-air resonances. Curves (a) and (b) are typical of the recordings of N made with the majority of ordinary samples. In contrast, curves (d) and (e) were obtained with foils deposited on highly HF-roughened substrates (approximately 1-min exposures), and curve (c) is representative of a class of ordinary samples which were obtained when the evaporation source ran out of Ag before the intended completion of the deposition. This last evidence suggests that comparatively hotter atoms, generated as the boat ran dry, contributed to the formation of a rougher surface.

A possible indication of the magnitude of the surface roughness can be obtained on the basis of Fedders's[15] calculation which relates the amplitude and periodicity of surface roughness components to the change in normal incidence reflectivity due to the surface-plasmon mode. The surface is assumed to satisfy the equation

$$z+\sum_n a_n \sin(\mathbf{k}_n\cdot\mathbf{r}+\alpha_n)=0, \tag{8}$$

where a_n, $\mathbf{k}_n$, and α_n are the amplitude, wave vector, and phase, respectively, of the nth roughness component, and $\mathbf{r}$ is a position vector in the x-y plane. In the approximation that only the component of wave vector k equal to that of the surface plasmon contributes, the expression for the integrated change in reflectivity becomes

$$\Delta E=2\pi a^2 k k_0, \tag{9}$$

where k_0 is the wave vector of the light and ΔR is defined by Eq. (1), Ref. 15.

An estimate of ΔR in the present case can be obtained from Fig. 7 by assuming that the solid curve would match the dashed curve in the absence of the surface-plasmon resonance. For $\Delta R=0.006$, $k=1\times10^6$ cm^{-1}, and $k_0=1.8\times10^5$ cm^{-1}, the resulting roughness amplitude is $a=8$ Å. This would seem to be quite reasonable for unannealed, rapidly deposited films.

E. Dielectric Constants

As indicated in Ref. 21, the polarization modulation technique is applicable to the problem of ellipsometry: With basically the same optical system shown in Fig. 1, it is also possible to measure a second parameter which is related to the relative phase shift between orthogonal components of the reflected light. Knowledge of these two independent quantities enables one to solve for the dielectric constants ϵ_1 and ϵ_2 by inversion of Fresnel's equations.[29]

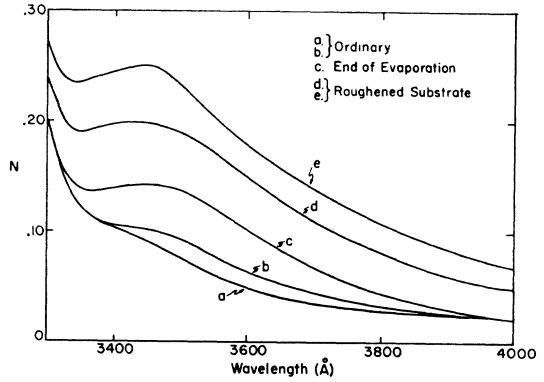

FIG. 11. Influence of experimental conditions on resonance strength: Ag-air interface.

[29] M. Born and E. Wolf, *Principles of Optics* (The Macmillan Co., New York, 1964), p. 620.

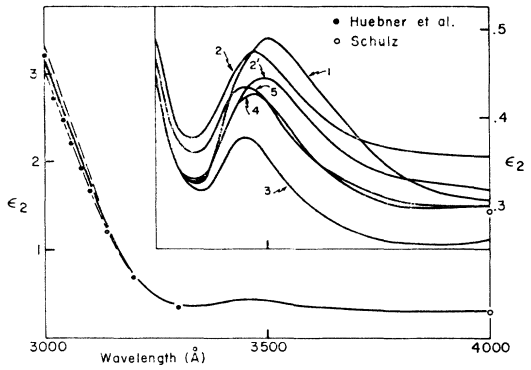

FIG. 12. Experimentally determined ϵ_2: 3000–4000 Å.

Implicit in this derivation is the approximation that the complex dielectric constant is a local function of position; that is, the response of the reflecting medium at a given point depends only upon the field applied at that point. Evidently this will not be valid at the energy of the surface-plasmon excitation, since that mode contributes to the response only at the surface of the foil. This approximation likewise breaks down at energies farther below the bulk plasmon energy in the anomalous skin-effect region.[30] However, ϵ_1 and ϵ_2 as derived from Fresnel's Equations are still well-defined quantities in terms of the experimentally determined parameters, and in order to intercompare the results of several measurements, as well as to compare this work with other optical studies, it is useful to present the data in terms of these customary functions.

Five Ag samples were prepared for this phase of the experiment by the usual method of vapor deposition on untreated glass substrates. In the interest of sample uniformity, all were made 4000 Å thick at rates of approximately 100 Å per sec, and pairs of samples were made simultaneously: Namely, samples 1 and 2 were made during the same evaporation, as were 3 and 4. The ellipsometry data from each sample were obtained within 3 days of its preparation; when not being used in an experiment, the samples were stored in a desiccator. Two sets of data, taken on two different days, were obtained from sample 2, and the label 2′ will be used to distinguish the second set from the first. Approximately 2 h were required to obtain a complete set of data, which consisted of recordings of N and either the sine or cosine of the relative phase angle, plus several sets of calibration measurements at fixed wavelengths. The wavelength range of this experiment, 3000–6000 Å, was chosen to include portions of both the free-electron and interband transition regions.

The resulting graphs of ϵ_2 are shown in Figs. 12 and 13; also included for comparison are data obtained by Huebner *et al.*[19] and Schulz.[31] For clarity, only the graph from one sample (5) appears in the lower portion of Fig. 12, with dashed lines indicating the envelope of curves for all other samples. The inset contains a magnified view of all six graphs of ϵ_2 in the region between 3250 and 4000 Å. Similarly, Fig. 13 shows all graphs in the range 4000–6000 Å. The striking feature of both figures is the large variation in ϵ_2 among samples which were intended to be uniform in their properties. Even graphs 2 and 2′ are markedly different, although sample age is presumably the only distinction between them.

Experimental uncertainties can account for little of these variations. Noise in the measurement of the ellipsometric parameters results in a 1% standard deviation of the locus of calculated values from the smooth curves presented above. Wavelength-dependent symmetric errors are no more than 4 to 6% over the entire range. Although the angle of incidence was uncertain by an estimated $\pm 1°$, particular care was exercised to ensure that θ was the same for each measurement. Indirect evidence discussed shortly indicated that the variation was at most $\pm\frac{1}{3}°$, which would account for less than one-quarter of the magnitude difference between graphs of ϵ_2. Also, uncertainty in θ is a wavelength-independent systematic error which simply puts the vertical placement of the curves in doubt by a uniform 10% per degree.

Therefore, both the differences in wavelength dependence and the width of the envelope of graphs must be taken as real effects, due almost entirely to variations in N of 30 to 40% between samples. In contrast the relative phase angle measurement showed little change from one sample to the next. This latter observa- observation established an upper limit on inadvertent variations in θ, since changes of $\pm\frac{1}{3}°$ would account for the average phase angle differences to the exclusion of all other effects.

The surface-plasmon contribution to the dielectric response occurs as a well-defined resonance in all graphs of ϵ_2 (inset, Fig. 12). Displayed in this fashion, its presence is considerably enhanced, owing to the relative

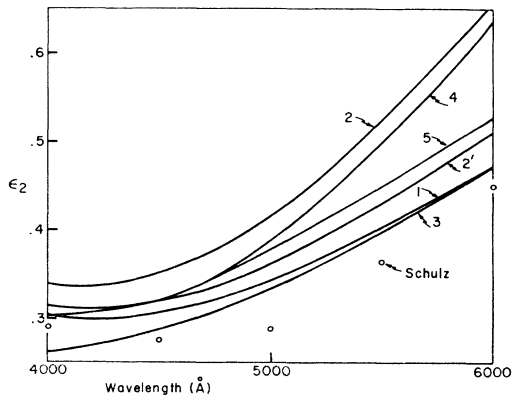

FIG. 13. Experimentally determined ϵ_2: 4000–6000 Å.

[30] K. L. Kliewer and R. Fuchs, Phys. Rev. **172**, 607 (1968).
[31] L. G. Schulz, J. Opt. Soc. Am. 44, 357 (1954); L. G. Schulz and F. R. Tangherlini, *ibid.* 44, 362 (1954).

TABLE I. Peak wavelength versus sample age.

Sample	Age	Peak wavelength (Å)
5	½ h	3450
4	½ h	3475
2	1½ h	3475
3	1 day	3450
1	3 days	3500
2′	3 days	3500

flatness of the background. The resonance size, as with ϵ_2 data elsewhere, differs greatly from the sample to sample, rising 25 to 50% above the background level. A particularly interesting feature is the occurrence of the resonant peaks at different wavelengths between 3450 and 3500 Å. Table I indicates the dependence of peak wavelength on the sample age, the age being measured from the time of evaporation to the beginning of the experiment.

These data illustrate that in general the resonance position relaxes toward longer wavelengths with increasing sample age, which is consistent with the expectation that a surface corrosion layer will begin to form as soon as the sample is prepared, changing the resonant condition according to Eq. 5. The fact that samples less than 2 h old exhibit different peak wavelengths demonstrates that initially this is a rather rapid effect, as well as a seemingly random one (note that resonance 4 was shifted more in 1½ h than 3 was in 1 day, although they were prepared simultaneously). Therefore, there exists considerable likelihood that, even before the samples have been removed from the evaporation chamber, the plasmon resonance has been relaxed several angstroms by a thin oxide or sulfide layer.

This conclusion is also implied by the ϵ_1 data plotted in Fig. 14. As in Fig. 12, the solid line is the graph for one sample (5), with the dashed lines indicating the envelope of ϵ_1 for all other samples. Values due to Huebner *et al.* and Schulz are shown as solid and open circles, respectively. Uncertainties are the same as those quoted for the ϵ_2 data, except that the wavelength-dependent systematic errors are only 2% in this case.

From these data, we find that $\epsilon_1 = -1.3$ at 3450 Å and that $\epsilon_1 = -2.1$ at 3600 Å, both in disagreement with earlier results. An 8% upward shift of these data, which is well within the limits of uncertainty in θ of $\pm 1°$, brings ϵ_1 up to its anticipated value of -1.9 at 3600 Å and improves agreement with the Schulz data between 4000–6000 Å. However, the unshifted resonance condition $\epsilon_1 = -1.0$ still occurs no higher than 3400 Å. The 25% upward shift required to make $\epsilon_1 = -1.0$ at 3450 Å is inconsistent with the limits of uncertainty on θ, the results of resonant relaxation due to a dielectric layer, and the data presented by Schulz. Therefore, we conclude that the resonance condition is satisfied at 3400 Å for a Ag-vacuum interface, and that it quickly relaxes by at least 50 Å when the foil is exposed to the atmosphere. As indicated in Sec. III A, this would imply a surface layer of approximately 20 Å thickness, assuming that $\epsilon_d \simeq 2$.

Final measurements of the ellipsometric parameters were made at two different angles of incidence, 30° and 60°, to see if the nonlocality of the dielectric function in the surface-plasmon region can be directly observed in ϵ_2. If Fresnel's equations describe the response of the Ag surface accurately, the dielectric functions computed at the two angles should agree exactly. Any significant nonlocal contribution to ϵ_2 might be expected to produce a θ-dependent correction. Surprisingly, no such discrepancy was observed: The magnitude of variations between the two ϵ_2 curves was only 2% over the wavelength range covered (3250 to 4000 Å) when corrected for a 12% uniform shift of one curve relative to the other due to the combined errors in the assigned values of the angles of incidence. This is true in spite of the fact that approximately ⅓ of the absorption at the peak of the surface-plasmon resonance is due to an excitation which must be described by a nonlocal dielectric function.

IV. SUMMARY

In summary of the preceding results, we have demonstrated that the surface-plasmon mode contributes measurably to the optical properties of thick Ag foils, even when considerable effort is made to prepare foils of high optical quality. A series of optical experiments established that the excess absorption was indirect in nature and that, of the several indirect mechanisms considered, only surface roughness enabled significant photon–surface-plasmon coupling. Although the effect of impurities was ignored in this work, it is anticipated on the basis of Fedders's remarks[15] that a suitable impurity concentration near the foil surface will also enable measurable coupling.

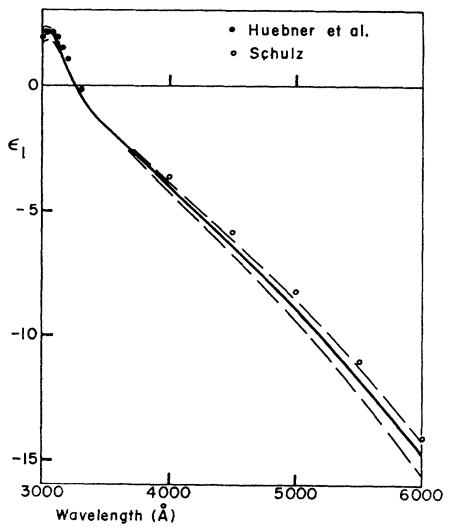

FIG. 14. Experimentally determined ϵ_1.

The surface-plasmon absorption is readily apparent in graphs of ϵ_2 computed from ellipsometry data, and the resonant wavelength is observed to relax to progressively longer wavelengths as the age of the foil increases. This provides a sensitive measure of the formation of a surface corrosion layer as a function of time and environmental conditions. On the basis of computed values of ϵ_1, it is concluded that the Ag-vacuum resonant wavelength is approximately 3400 Å; in contrast, the resonant wavelength is always greater than or equal to 3450 Å after exposure of the foil to the atmosphere.

ACKNOWLEDGMENTS

The authors are indebted to Professor J. J. Hopfield and Professor P. A. Fedders for many useful suggestions and stimulating discussions throughout the course of this work.

PHYSICAL REVIEW VOLUME 188, NUMBER 2 10 DECEMBER 1969

Lattice Thermal Conductivity of Superconducting Niobium Carbide*

LEE G. RADOSEVICH†
Department of Physics and Materials Research Laboratory, University of Illinois, Urbana, Illinois 61801

AND

WENDELL S. WILLIAMS
Department of Physics, Department of Ceramic Engineering, and Materials Research Laboratory, University of Illinois, Urbana, Illinois 61801

(Received 22 August 1969)

The unusually low lattice thermal conductivity of the transition-metal carbides at low temperatures has been attributed to the scattering of phonons by conduction electrons. An experiment which confirms this interpretation is reported. Thermal conductivity measurements on single-crystal $NbC_{0.96}$ through its superconducting critical temperature (9.8°K) show that the lattice component of the thermal conductivity, K_{ls}, increases greatly below T_c because of decreased phonon-electron scattering. The maximum increase in lattice thermal conductivity from this effect occurs at 3°K with K_{ls}/K_{ln} equal to 160. The theories of Bardeen, Rickayzen, and Tewordt and of Klemens and Tewordt for the influence of electrons and point defects on lattice conductivity provide a quantitative interpretation of the effect. The best fit to the $NbC_{0.96}$ data is for $2\epsilon(o)/kT_c=4.0$. The behavior of $NbC_{0.96}$ is in contrast to that of $NbC_{0.76}$, which remains in the normal state throughout the temperature interval studied and shows no increase in thermal conductivity.

I. INTRODUCTION

PREVIOUS measurements[1,2] of the thermal conductivity of Groups IV and V transition-metal carbides have shown that strong phonon-electron scattering must be invoked to explain the low-temperature behavior of the lattice thermal conductivity. It was also noted, however, that the ordinary theory of phonon-electron scattering does not apply to carbide samples which are highly carbon deficient. Hence, some experimental demonstration of the above interpretation was sought.

In this paper, we report measurements on the thermal conductivity of superconducting niobium carbide which do demonstrate experimentally the existence of strong phonon-electron scattering in the transition-metal carbides. Use is made of the fact that some of the carbides have superconducting critical temperatures in the range of interest. Since electrons in the superconducting state do not scatter phonons, an increase in lattice conductivity below T_c is predicted and observed. A comparison of the data with the theories of Bardeen, Rickayzen, and Tewordt[3] (BRT) and Klemens and Tewordt[4] (KT) shows quantitative agreement for the effect of phonon-electron scattering and point-defect scattering on the lattice thermal conductivity.

II. EXPERIMENTAL

Two specimens of single-crystal niobium carbide, $NbC_{0.76}$ [5] and $NbC_{0.96}$,[6] were studied. The specimens, which crystallize in the rocksalt structure, are carbon

* Work supported in part by the U. S. Atomic Energy Commission under Contract No. AT(11-1)-1198.

† Present address: Sandia Laboratories, Livermore, Calif. 94550.

[1] L. G. Radosevich and W. S. Williams, Phys. Rev. **181**, 1110 (1969).

[2] L. G. Radosevich and W. S. Williams (to be published).

[3] J. Bardeen, G. Rickayzen, and L. Tewordt, Phys. Rev. **113**, 982 (1959).

[4] P. G. Klemens and L. Tewordt, Rev. Mod. Phys. **36**, 118 (1964).

[5] This specimen has been characterized in (1).

[6] This specimen was obtained from Ventron Electronics Corporation, Alfa Crystals Division. The carbon-to-metal ratio of 0.96 was determined from measurements of the superconducting transition temperature T_c and comparison with data of Toth *et al.* See L. E. Toth, M. Ishikawa, and Y. A. Chang, Acta Met. **16**, 1183 (1968).